Accepted to *International Journal of Applied Nonlinear Science*

Convergence Analysis of a Heuristic Collective Sphere Packing Algorithm

Author names and affiliations
Yanheng Li
Department of Mechanical, Aerospace, and Nuclear Engineering
Rensselaer Polytechnic Institute
110 8th street
Troy, New York, USA
liy19@rpi.edu

Wei Ji* (Corresponding author)
Department of Mechanical, Aerospace, and Nuclear Engineering
Rensselaer Polytechnic Institute
110 8th street
Troy, New York, USA
Tel: 1-(518)2766602
Fax: 1-(518)2766025
jiw2@rpi.edu

Abstract

Computer simulation of random sphere packing is important for the study of densely packed particulate systems. In previous work, Quasi Dynamics Method (QDM), a heuristic collective random sphere packing algorithm was developed to effectively handle large numbers of densely packed spheres in complex geometries. In this work, a theoretical analysis of the convergence of QDM is performed and the impact of algorithm step size on the convergence is discussed. System potential functions that measure the overall system overlaps are introduced and defined. By using different system potentials, the convergence/stability of QDM for a sphere packing domain with and without active boundary conditions is investigated. QDM is proved to be strictly convergent with small step size when no active boundary constraint exists. When active boundary constraint is imposed, important results such as the upper limit of step size for convergence and selection criteria for step size are also theoretically obtained. Our analyses focus on systems packed with mono-dispersed spheres. The mathematical approaches for the analysis, however, can be easily modified for poly-dispersed sphere systems and extended to analyze other collective packing algorithms.

Keywords: random sphere packing; collective dynamics method; stability and convergence; boundary constraints; granular flow simulation

1. Introduction

Random sphere packing has been an active research topic for a long time [1-7]. It plays

important roles in simulating and understanding fundamental physical phenomena in many scientific and engineering systems with granular materials [8-12]. Typical randomly-packed sphere (particle) systems consist of large quantities of spherical solid particles [11-12]. In addition to necessary experimental and analytical studies, computational modeling of these applications is indispensable in exploring their mechanical and chemical properties. However, great computational challenges exist due to the large particle quantity and ubiquitous non-continuous contact/collisions among particles in these applications which make the typical simulation approach (such as Discrete Element Methods, or DEM) very inefficient [13]. Therefore for a specific problem, it is very important to start the simulation at a packing arrangement that is close to the target arrangement so as to reduce the transition time from the initial state to the target state, which calls for an efficient initial packing algorithm that can generate any required initial state of particles within the specified geometry [5].

In previous work, a heuristic collective method (Quasi-Dynamics Method, or QDM) [5] has been developed to pack mono- and poly-dispersed spheres with applications to the initial packing arrangement for general granular material systems with up to millions of highly packed spherical particles. In QDM, the positions of spheres are first uniformly sampled allowing inter-sphere overlaps. Then, an iterative heuristic overlap elimination process is applied based on the inter-sphere overlap and a simplified linear normal contact force model. It has been shown that the developed method can successfully provide fast packing for complex container geometries at various packing fractions (from 30% to the random close packing limit which is around 64% [14]). This method can be extended to analyze general granular flow simulations by providing an efficient initial and static random sphere packing configuration in the system, which is very close to the equilibrium state of the system (steady state with momentum and energy balance). Since the equilibrium state of granular materials presents a realistic configuration in many industrial applications such as hopper flow and the thermodynamic balance of dense colloidal suspensions, QDM can benefit the study of granular materials by efficiently providing a close-to-reality equilibrium state at designated packing densities, which can significantly reduce the computation time for granular flow simulation under realistic modeling.

Successful demonstration of QDM has been performed and guidelines for choosing algorithm parameters have been provided based on numerical simulations [5]. However, some important properties, such as the convergence rate, the impact of step size and packing fraction on the algorithm performance, are still unclear, due to the complicated discontinuous formulation of the overlap function. Understanding these properties is a key for predicting the algorithm convergence performance (especially for large granular systems) and identifying its applicability for different applications. This is important for the utilization of not only QDM, but also other similar collective overlap-eliminating packing algorithms. By exploring QDM's stability and convergence properties in a rigorously analytical way, the governing laws behind these properties can be fully understood.

Besides inter-sphere interactions, a container (boundary) can also exert "force" onto spheres if there is an overlap between them. Therefore, we divide studied sphere packing systems into

two categories: (1) packing systems without active boundary constraints (no boundary at all or the boundary is much larger than the outreach of the packing and hence not active), and (2) packing systems with active boundary constraints. In this work, the strict convergence proof for the unconstrained case is obtained first. As for packing with active boundary constraints, by exploring the stability of QDM using a general convex analysis approach, an upper bound function with a simpler formulation than the original overlap function is obtained. Based on this simplified objective function, numerical behaviors of QDM are interpreted and predicted. Since most of the derivation and analysis is based on general linear algebra and convex analysis which is independent of the specific algorithm, this analytical approach can be extended to other collective overlap-eliminating sphere packing algorithms such as the algorithm proposed by Clarke [2] where the convergence performance has not yet been systematically discussed.

2. Algorithm Description

In the QDM, spheres are initially positioned by the uniform sampling of sphere center positions over the container without any constraints. After that, sphere overlaps are widely present due to the finite volume of each sphere and the container. For each sphere, an artificial normal contact force is introduced that is associated with its overlaps with other spheres. The force is calculated as a summation of all inter-sphere overlap vectors. Based on the calculated artificial normal contact force, a sphere is moved along the direction of the force and the moving distance is determined both by the magnitude of the force and the algorithm step size. This overlap-eliminating approach is performed iteratively until all the inter-sphere overlaps are completely eliminated. Compared with Clarke's approach where a sphere movement will be accepted only when the maximum inter-sphere overlap is not increased and the spheres are moved sequentially, QDM does not reject any move and all the spheres are moved collectively which is more consistent with the realistic contact mechanics of granular materials. In the original QDM, the boundary constraint is enforced by introducing a wall-sphere normal contact force that is proportional to the overlap between the wall and sphere to eliminate any boundary violation iteratively. In the present work, a simplified projection approach is used to impose the boundary condition for every step, i.e., if a sphere moves out of the boundary after a move, a projection operation is performed to pull the sphere back such that the sphere just touches the boundary. The detailed procedure of the QDM is described below.

Assume that container geometry, total number of spheres N and sphere radius distribution are given. Denote $\boldsymbol{X}_i$ (i=1, 2, …, N) as the center position (vector) of i^{th} sphere. The origin of the reference frame is usually centered in the container, therefore the boundary constraints $\boldsymbol{C}$ can be expressed as

$$\boldsymbol{C} \subset \mathbb{R}^{3n}: \qquad X_i \in \boldsymbol{C} \quad i = 1,2,...N \tag{1}$$

The distance between the i^{th} and j^{th} spheres S_i and S_j can be expressed as $d_{ij} = ||\boldsymbol{X}_i - \boldsymbol{X}_j||$. It is clear that there is an overlap between the two spheres only when $d_{ij} < r_i + r_j$, and the overlap depth δ_{ij} can be expressed as:

$$\delta_{ij} = \max(r_i + r_j - d_{ij}, 0). \tag{2}$$

For a mono-dispersed situation, this can be written as:

$$\delta_{ij} = \max(2r - d_{ij}, 0). \tag{3}$$

Hereafter a simplified notation $\max_0(a) = \max(a,0)$ will be used. Denote $\boldsymbol{\delta}_i$ as the summation of all inter-sphere overlap vectors for the ith sphere:

$$\boldsymbol{\delta}_i = \sum_{j \in M_i} \delta_{ij} \boldsymbol{n}_{ij} = \boldsymbol{F}_i, \tag{4}$$

where $\boldsymbol{n}_{ij}=(\boldsymbol{X}_i-\boldsymbol{X}_j)/d_{ij}$. In order to give this summed vector a clear physical interpretation, we use $\boldsymbol{F}_i$ to equivalently represent the summed overlap vector, meaning the net force exerted onto the ith sphere.

According to QDM, the displacement (vector) for ith sphere is proportional to the summed overlap vector, or the net force, for sphere i:

$$\Delta \boldsymbol{X}_i = \alpha \boldsymbol{F}_i = \alpha \boldsymbol{\delta}_i, \tag{5}$$

where α is the step size.

Define $\boldsymbol{\delta}_{ij}=\delta_{ij}\boldsymbol{n}_{ij}$ as the overlap vector between the ith and jth sphere. Because $\boldsymbol{\delta}_{ij}=-\boldsymbol{\delta}_{ji}$, there is:

$$\sum_{i=1}^{N} \boldsymbol{\delta}_i = \sum_{i=1}^{N} \boldsymbol{F}_i = 0, \tag{6}$$

which can be interpreted as the zero total external force of the system. Denote $\boldsymbol{X}_i^{(k)}$ as the center position of the ith sphere at the k^{th} step. For the k+1th step, it is possible that the new position $\boldsymbol{Z}_i^{(k+1)}$ after one move, which satisfies

$$\boldsymbol{Z}_i^{(k+1)} = \boldsymbol{X}_i^{(k)} + \Delta \boldsymbol{X}_i^{(k)}, \tag{7}$$

may not satisfy the boundary constraints. Therefore a projection operation $P(\bullet)$ is applied to "pull" $\boldsymbol{Z}_i^{(k+1)}$ back into the feasible domain $\boldsymbol{C}$:

$$\boldsymbol{X}_i^{(k+1)} = P(\boldsymbol{Z}_i^{(k+1)}) = P(\boldsymbol{X}_i^{(k)} + \Delta \boldsymbol{X}_i^{(k)}). \tag{8}$$

For example, in a box container, the projection operation is quite easy to understand. Let $\tilde{X}_{i,m}$ and $X_{i,m}$ (j=1,2,3) denote the three components of sphere center position, before and after the projection operation respectively. Then the projection operator can be interpreted as:

$$X_{i,m} = \begin{cases} \tilde{X}_{i,m}, & \tilde{X}_{i,m} \le L/2 - r, \\ L/2 - r, & \tilde{X}_{i,m} > L/2 - r. \end{cases} \tag{9}$$

3. Algorithm Analysis

As an iterative numerical algorithm, it is necessary to explore the convergence performance

to better understand and utilize the algorithm for practical applications. The key question for convergence analysis is: will the algorithm converge to an overlap-free configuration $\boldsymbol{X}^*$ (convergence)? Or, from a more general and less strict point of view, for any initial state $\boldsymbol{X}^{(1)}$, will the overall overlap be confined within a finite small value as the algorithm proceeds (stability)? This section provides stability and convergence analyses for the algorithm and important results such as the upper bound function for the system potential and guidelines for choosing step sizes are provided based on the analyses.

Since QDM is an iterative overlap eliminating algorithm, a function to measure the overall system overlap is needed to indicate current extent of overlap and when to stop the algorithm [15]. Here we propose three system potential functions to serve as the measure of overall overlap. The stability analysis is based on the basic properties of the QDM and these potential functions.

No matter which boundary constraint is imposed: unconstrained or constrained, after each iteration step, only sphere-sphere overlaps exist (the projection operation for constrained case enforces the overlap between sphere and wall to be zero). Therefore, system potential functions are only related to sphere-sphere overlaps and these are defined as follows.

The type 1 potential function is defined as:

$$V_1(\boldsymbol{X}) = \sum_{i=1}^{N-1}\sum_{j>i}^{N} \delta_{ij} = \sum_{i=1}^{N-1}\sum_{j>i}^{N} \max_0(2r - d_{ij}), \tag{10}$$

where $\boldsymbol{X} = (\boldsymbol{X}_1^{\mathrm{T}}\ \boldsymbol{X}_2^{\mathrm{T}}\ \boldsymbol{X}_3^{\mathrm{T}}\ \ldots\ \boldsymbol{X}_{\mathrm{N}}^{\mathrm{T}})^{\mathrm{T}}$ is a $3N$ by 1 vector that records all the sphere positions at each iteration step in the QDM.

Similarly, we can define the type 2 potential function as:

$$V_2(\boldsymbol{X}) = \sum_{i=1}^{N-1}\sum_{j>i}^{N} \delta_{ij}^{\ 2}. \tag{11}$$

And the type d potential function:

$$V_{\mathrm{d}}(\boldsymbol{X}) = \sum_{i=1}^{N-1}\sum_{j>i}^{N} \delta_{ij} d_{ij}. \tag{12}$$

All above potential functions are positive and definite. They decrease as the overall system overlap decrease. Therefore, they can serve as a measure of the overall system overlaps. If we denote $\boldsymbol{X}^*$ as the position vector at an overlap-free state, then $V(\boldsymbol{X}^*) = 0$ is the global minimum value of $V(\boldsymbol{X})$.

3-1 Convergence of unconstrained situation

Before the stability proof for the general constrained situation, we start with the unconstrained condition to show that QDM is convergent when boundary conditions are not imposed, i.e. spheres do not touch the boundary after each move, which has many

applications such as the diffusion of colloidal particles in large water body. For unconstrained situation, the effective volume fraction of the sphere assembly, which is the total sphere volume divided by the smallest possible convex container that contains all the spheres, can be controlled by initially sampling the sphere center locations within a virtual boundary that is far away from the realistic boundary. As for the proof of the packing with active boundary constraints, it follows a different procedure but shares many properties of the potential functions proposed in the unconstrained case.

To start the proof, we need the following important lemma.

Lemma 1: $\sum_{i=1}^{N}\langle \boldsymbol{\delta}_{\mathrm{i}}, \boldsymbol{X}_{\mathrm{i}}\rangle = \sum_{i=1}^{N\text{-}1}\sum_{j>i}^{N}\left\langle \delta_{\mathrm{ij}}\frac{\boldsymbol{X}_{\mathrm{i}}-\boldsymbol{X}_{\mathrm{j}}}{d_{\mathrm{ij}}}, \boldsymbol{X}_{\mathrm{i}}-\boldsymbol{X}_{\mathrm{j}}\right\rangle = \sum_{i=1}^{N\text{-}1}\sum_{j>i}^{N}\delta_{\mathrm{ij}}d_{\mathrm{ij}} = V_{\mathrm{d}}$, where <·> is the Euclidean inner product operator.

Proof:
Denote $\boldsymbol{\delta}_M$ as an N by 3N matrix with $\boldsymbol{\delta}_{\mathrm{ij}}{}^T$ occupying its i$^{\mathrm{th}}$ row and 3(j-1) to 3j columns:

$$\boldsymbol{\delta}_M = \begin{pmatrix} \boldsymbol{\delta}_{11}{}^T & \cdots & \boldsymbol{\delta}_{1N}{}^T \\ \vdots & \ddots & \vdots \\ \boldsymbol{\delta}_{N1}{}^T & \cdots & \boldsymbol{\delta}_{NN}{}^T \end{pmatrix},$$

where $\boldsymbol{\delta}_{\mathrm{ij}}{}^T = \boldsymbol{0}^T = [0\ 0\ 0]$ for any i and j. There is a decomposition about $\boldsymbol{\delta}_M$:

$$\boldsymbol{\delta}_M = \begin{pmatrix} \boldsymbol{\delta}_{11}{}^T & \cdots & \boldsymbol{\delta}_{1N}{}^T \\ \vdots & \ddots & \vdots \\ \boldsymbol{\delta}_{N1}{}^T & \cdots & \boldsymbol{\delta}_{NN}{}^T \end{pmatrix} = \begin{pmatrix} \boldsymbol{0}^T & \cdots & \boldsymbol{0}^T \\ \boldsymbol{\delta}_{21}{}^T & \ddots & \vdots \\ \vdots & & \\ \boldsymbol{\delta}_{N1}{}^T \cdots & \boldsymbol{\delta}_{N,N-1}{}^T & \boldsymbol{0}^T \end{pmatrix} + \begin{pmatrix} \boldsymbol{0}^T & \boldsymbol{\delta}_{12}{}^T \cdots & \boldsymbol{\delta}_{1N}{}^T \\ & & \vdots \\ \vdots & \ddots & \\ & & \boldsymbol{\delta}_{N-1,N}{}^T \\ \boldsymbol{0}^T & \cdots & \boldsymbol{0}^T \end{pmatrix}$$

$$= \boldsymbol{\delta}_M^L + \boldsymbol{\delta}_M^U.$$

Denote $\boldsymbol{X}_{\mathrm{M}}$ as a 3N by N matrix with the expression:

$$\boldsymbol{X}_M = \begin{pmatrix} \boldsymbol{X}_1 & \cdots & \boldsymbol{X}_N \\ \vdots & \ddots & \vdots \\ \boldsymbol{X}_1 & \cdots & \boldsymbol{X}_N \end{pmatrix}.$$

Then there is

$$\begin{aligned} \sum_{i=1}^{N}\langle \boldsymbol{\delta}_{\mathrm{i}}, \boldsymbol{X}_{\mathrm{i}}\rangle &= \sum_{i=1}^{N}\left\langle \sum_{\substack{j=1 \\ j\neq i}}^{N}\boldsymbol{\delta}_{\mathrm{ij}}, \boldsymbol{X}_{\mathrm{i}}\right\rangle \\ &= tr(\boldsymbol{\delta}_M\boldsymbol{X}_M) \\ &= tr(\boldsymbol{\delta}_M^L + \boldsymbol{\delta}_M^U)\boldsymbol{X}_M) \\ &= tr(\boldsymbol{\delta}_M^L\boldsymbol{X}_M + \boldsymbol{\delta}_M^U\boldsymbol{X}_M). \end{aligned}$$

By using the additivity of trace function "*tr*", we can rewrite above equality as:

$$\sum_{i=1}^{N}\langle \boldsymbol{\delta}_{\mathrm{i}}, \boldsymbol{X}_{\mathrm{i}}\rangle = tr(\boldsymbol{\delta}_M^L \boldsymbol{X}_M) + tr(\boldsymbol{\delta}_M^U \boldsymbol{X}_M)$$

$$= \sum_{i=1}^{N\text{-}1}\sum_{j>i}^{N}\langle \boldsymbol{\delta}_{\mathrm{ij}}, \boldsymbol{X}_{\mathrm{i}}\rangle + \sum_{i=1}^{N\text{-}1}\sum_{j>i}^{N}\langle \boldsymbol{\delta}_{ji}, \boldsymbol{X}_{\mathrm{j}}\rangle$$

$$= \sum_{i=1}^{N\text{-}1}\sum_{j>i}^{N}\langle \boldsymbol{\delta}_{\mathrm{ij}}, \boldsymbol{X}_{\mathrm{i}} - \boldsymbol{X}_{\mathrm{j}}\rangle$$

$$= \sum_{i=1}^{N\text{-}1}\sum_{j>i}^{N}\left\langle \delta_{\mathrm{ij}}\frac{\boldsymbol{X}_{\mathrm{i}} - \boldsymbol{X}_{\mathrm{j}}}{d_{\mathrm{ij}}}, \boldsymbol{X}_{\mathrm{i}} - \boldsymbol{X}_{\mathrm{j}}\right\rangle$$

$$= \sum_{i=1}^{N\text{-}1}\sum_{j>i}^{N}\frac{\delta_{\mathrm{ij}}}{d_{\mathrm{ij}}}\langle \boldsymbol{X}_{\mathrm{i}} - \boldsymbol{X}_{\mathrm{j}}, \boldsymbol{X}_{\mathrm{i}} - \boldsymbol{X}_{\mathrm{j}}\rangle$$

$$= \sum_{i=1}^{N\text{-}1}\sum_{j>i}^{N}\frac{\delta_{\mathrm{ij}}}{d_{\mathrm{ij}}}d_{\mathrm{ij}}^{\,2} = \sum_{i=1}^{N\text{-}1}\sum_{j>i}^{N}\delta_{\mathrm{ij}}d_{\mathrm{ij}} = V_{\mathrm{d}} \geq 0.$$

Lemma 1 relates the summed overlap vector and sphere position in the inertial frame with the inter-sphere overlap and inter-sphere distance which are independent of the reference frame. It is worth mentioning that Lemma 1 does not use any specific QDM property. Therefore this lemma represents the general feature of packed sphere systems with overlaps independent of the packing algorithm. More importantly, Lemma 1 clearly indicates that if all the summed overlaps are equal to zero ($\boldsymbol{\delta}_{\mathrm{i}} = 0$ for all i), then all the inter-sphere overlaps are equal to zero ($\sum_{i=1}^{N\text{-}1}\sum_{j>i}^{N}\delta_{\mathrm{ij}}d_{\mathrm{ij}} = 0 \Leftrightarrow \delta_{\mathrm{ij}} = 0$). Without resorting to Lemma 1, this intuitive result cannot be easily obtained by solving $\boldsymbol{\delta}_i = \sum_{j\in M_i}\delta_{\mathrm{ij}}\boldsymbol{n}_{\mathrm{ij}} = \mathbf{0}$ (for i=1, 2, …, N), because from Eq. (6), the matrix related to the linear equations is not full rank and hence the solution is not unique.

In the proof of convergence for the unconstrained case, we use the d-potential function V_{d} as the measure of the overall system overlap. The difference between the d-potential functions at the k+1$^{\mathrm{th}}$ and k^{th} step can be written as:

$$V_{\mathrm{d}}^{(k+1)} - V_{\mathrm{d}}^{(k)} = \sum_{i=1}^{N\text{-}1}\sum_{j>i}^{N}\delta_{\mathrm{ij}}^{(k+1)}d_{\mathrm{ij}}^{(k+1)} - \sum_{i=1}^{N\text{-}1}\sum_{j>i}^{N}\delta_{\mathrm{ij}}^{(k)}d_{\mathrm{ij}}^{(k)}. \quad (13)$$

By using Lemma 1 and the QDM principle, Eq. (13) can be rewritten as:

$$
\begin{aligned}
& V_{\mathrm{d}}^{(k+1)} - V_{\mathrm{d}}^{(k)} \\
&= \sum_{i=1}^{N} \left\langle \boldsymbol{\delta}_{\mathrm{i}}^{(k+1)}, \boldsymbol{X}_{\mathrm{i}}^{(k+1)} \right\rangle - \sum_{i=1}^{N} \left\langle \boldsymbol{\delta}_{\mathrm{i}}^{(k)}, \boldsymbol{X}_{\mathrm{i}}^{(k)} \right\rangle \\
&= \sum_{i=1}^{N} \left\langle \boldsymbol{\delta}_{\mathrm{i}}^{(k+1)}, \boldsymbol{X}_{\mathrm{i}}^{(k)} + \alpha \boldsymbol{\delta}_{\mathrm{i}}^{(k)} \right\rangle - \sum_{i=1}^{N} \left\langle \boldsymbol{\delta}_{\mathrm{i}}^{(k)}, \boldsymbol{X}_{\mathrm{i}}^{(k)} \right\rangle \\
&= \sum_{i=1}^{N} \left\langle \boldsymbol{\delta}_{\mathrm{i}}^{(k+1)} - \boldsymbol{\delta}_{\mathrm{i}}^{(k)}, \boldsymbol{X}_{\mathrm{i}}^{(k)} \right\rangle + \alpha \sum_{i=1}^{N} \left\langle \boldsymbol{\delta}_{\mathrm{i}}^{(k+1)}, \boldsymbol{\delta}_{\mathrm{i}}^{(k)} \right\rangle \\
&= \sum_{i=1}^{N\text{-}1} \sum_{j>i}^{N} \left\langle \boldsymbol{\delta}_{\mathrm{ij}}^{(k+1)} - \boldsymbol{\delta}_{\mathrm{ij}}^{(k)}, \boldsymbol{X}_{\mathrm{i}}^{(k)} - \boldsymbol{X}_{\mathrm{j}}^{(k)} \right\rangle + \alpha \sum_{i=1}^{N\text{-}1} \sum_{j>i}^{N} \left\langle \boldsymbol{\delta}_{\mathrm{ij}}^{(k)}, \boldsymbol{\delta}_{\mathrm{i}}^{(k+1)} - \boldsymbol{\delta}_{\mathrm{j}}^{(k+1)} \right\rangle \\
&= \Delta V_{[1]} + \Delta V_{[2]}
\end{aligned}
\quad . \tag{14}
$$

It can be seen in Eq. (14) that we decompose the difference of potentials at two contiguous steps into a first order term $\Delta V_{[1]}$ and a second order term $\Delta V_{[2]}$ which is positive during most of the steps. As we can see in Eq. (14), when the step size α is small enough, the first order term is dominant. Hence under this small step size assumption, we will analyze the first order term only. The upper limit for the step size will be discussed in general constrained situations.

Based on the definition of inter-sphere overlap, we can rewrite the expression for $\boldsymbol{\delta}_{\mathrm{ij}}$ as:

$$
\boldsymbol{\delta}_{\mathrm{ij}} = \tilde{d}_{\mathrm{ij}} \boldsymbol{n}_{\mathrm{ij}} - (\boldsymbol{X}_{\mathrm{i}} - \boldsymbol{X}_{\mathrm{j}}) , \tag{15}
$$

where $\tilde{d}_{\mathrm{ij}} = \begin{cases} 2r, & \delta_{\mathrm{ij}} > 0 \\ d_{\mathrm{ij}}, & \delta_{\mathrm{ij}} = 0 \end{cases}$. Then for the 1st order term, we can analyze it in three situations:

1) if $\delta_{\mathrm{ij}}^{(k)} > 0$, $\delta_{\mathrm{ij}}^{(k+1)} = 0$ then:

$$
\begin{aligned}
\Delta V_{[1]} \underset{\delta_{\mathrm{ij}}^{(k+1)}=0}{\delta_{\mathrm{ij}}^{(k)}>0,} &= \sum_{\delta_{\mathrm{ij}}^{(k)}>0} \sum_{\delta_{\mathrm{ij}}^{(k+1)}=0} \left\langle \boldsymbol{\delta}_{\mathrm{ij}}^{(k+1)} - \boldsymbol{\delta}_{\mathrm{ij}}^{(k)}, \boldsymbol{X}_{\mathrm{i}}^{(k)} - \boldsymbol{X}_{\mathrm{j}}^{(k)} \right\rangle \\
&= \sum_{\delta_{\mathrm{ij}}^{(k)}>0} \sum_{\delta_{\mathrm{ij}}^{(k+1)}=0} \left\langle d_{\mathrm{ij}}^{(k+1)} \boldsymbol{n}_{\mathrm{ij}}^{(k+1)} - 2r \boldsymbol{n}_{\mathrm{ij}}^{(k)}, d_{\mathrm{ij}}^{(k)} \boldsymbol{n}_{\mathrm{ij}}^{(k)} \right\rangle - \\
&\quad \sum_{\delta_{\mathrm{ij}}^{(k)}>0} \sum_{\delta_{\mathrm{ij}}^{(k+1)}=0} \left\langle (\boldsymbol{X}_{\mathrm{i}}^{(k+1)} - \boldsymbol{X}_{\mathrm{i}}^{(k)}) - (\boldsymbol{X}_{\mathrm{j}}^{(k+1)} - \boldsymbol{X}_{\mathrm{j}}^{(k+1)}), \boldsymbol{X}_{\mathrm{i}}^{(k)} - \boldsymbol{X}_{\mathrm{j}}^{(k)} \right\rangle \\
&= \sum_{\delta_{\mathrm{ij}}^{(k)}>0} \sum_{\delta_{\mathrm{ij}}^{(k+1)}=0} \left\langle d_{\mathrm{ij}}^{(k+1)} \boldsymbol{n}_{\mathrm{ij}}^{(k+1)} - 2r \boldsymbol{n}_{\mathrm{ij}}^{(k)}, d_{\mathrm{ij}}^{(k)} \boldsymbol{n}_{\mathrm{ij}}^{(k)} \right\rangle - \\
&\quad \alpha \sum_{\delta_{\mathrm{ij}}^{(k)}>0} \sum_{\delta_{\mathrm{ij}}^{(k+1)}=0} \left\langle \delta_{\mathrm{i}}^{(k+1)} - \delta_{\mathrm{i}}^{(k)}, \boldsymbol{X}_{\mathrm{i}}^{(k)} - \boldsymbol{X}_{\mathrm{j}}^{(k)} \right\rangle .
\end{aligned}
\tag{16}
$$

Similarly, there are:

2) if $\delta_{\mathrm{ij}}^{(k)} = 0$, $\delta_{\mathrm{ij}}^{(k+1)} > 0$ then:

$$\Delta V_{[1]}\underset{\substack{\delta_{ij}^{(k)}=0,\\ \delta_{ij}^{(k+1)}>0}}{=}\sum_{\delta_{ij}^{(k)}=0}\sum_{\delta_{ij}^{(k+1)}>0}\left\langle 2r^{(k+1)}\boldsymbol{n}_{ij}^{(k+1)}-d_{ij}^{(k)}\boldsymbol{n}_{ij}^{(k)},d_{ij}^{(k)}\boldsymbol{n}_{ij}^{(k)}\right\rangle-\alpha\sum_{\delta_{ij}^{(k)}=0}\sum_{\delta_{ij}^{(k+1)}>0}\left\langle\delta_i^{(k+1)}-\delta_i^{(k)},\boldsymbol{X}_i^{(k)}-\boldsymbol{X}_j^{(k)}\right\rangle. \tag{17}$$

3) if $\delta_{ij}^{(k)}>0$, $\delta_{ij}^{(k+1)}>0$ then:

$$\Delta V_{[1]}\underset{\substack{\delta_{ij}^{(k)}>0,\\ \delta_{ij}^{(k+1)}>0}}{=}\sum_{\delta_{ij}^{(k)}>0}\sum_{\delta_{ij}^{(k+1)}>0}\left\langle 2r\boldsymbol{n}_{ij}^{(k+1)}-2r\boldsymbol{n}_{ij}^{(k)},d_{ij}^{(k)}\boldsymbol{n}_{ij}^{(k)}\right\rangle-\alpha\sum_{\delta_{ij}^{(k)}>0}\sum_{\delta_{ij}^{(k+1)}>0}\left\langle\delta_i^{(k+1)}-\delta_i^{(k)},\boldsymbol{X}_i^{(k)}-\boldsymbol{X}_j^{(k)}\right\rangle. \tag{18}$$

Now we sum Eqs. (16-18) to obtain:

$$\begin{aligned}\Delta V_{[1]}&=\Delta V_{[1]}\underset{\substack{\delta_{ij}^{(k)}>0,\\ \delta_{ij}^{(k+1)}=0}}{+}\Delta V_{[1]}\underset{\substack{\delta_{ij}^{(k)}<0,\\ \delta_{ij}^{(k+1)}>0}}{+}\Delta V_{[1]}\underset{\substack{\delta_{ij}^{(k)}>0,\\ \delta_{ij}^{(k+1)}>0}}{}\\&=-\alpha\sum_{i=1}^{N-1}\sum_{j>i}^{N}\left\langle\boldsymbol{\delta}_i^{(k)}-\boldsymbol{\delta}_j^{(k)},\boldsymbol{X}_i^{(k)}-\boldsymbol{X}_j^{(k)}\right\rangle+\\&\sum_{\delta_{ij}^{(k)}>0}\sum_{\delta_{ij}^{(k+1)}=0}\left\langle 2r\boldsymbol{n}_{ij}^{(k+1)}-\tilde{d}_{ij}^{(k)}\boldsymbol{n}_{ij}^{(k)},d_{ij}^{(k)}\boldsymbol{n}_{ij}^{(k)}\right\rangle+\\&\sum_{\delta_{ij}^{(k)}=0}\sum_{\delta_{ij}^{(k+1)}>0}\left\langle d_{ij}^{(k+1)}\boldsymbol{n}_{ij}^{(k+1)}-2r\boldsymbol{n}_{ij}^{(k)},d_{ij}^{(k)}\boldsymbol{n}_{ij}^{(k)}\right\rangle+\\&\sum_{\delta_{ij}^{(k)}>0}\sum_{\delta_{ij}^{(k+1)}>0}\left\langle 2r\boldsymbol{n}_{ij}^{(k+1)}-2r\boldsymbol{n}_{ij}^{(k)},d_{ij}^{(k)}\boldsymbol{n}_{ij}^{(k)}\right\rangle.\end{aligned} \tag{19}$$

Because

$$\begin{aligned}&-\alpha\sum_{i=1}^{N-1}\sum_{j>i}^{N}\left\langle\boldsymbol{\delta}_i^{(k)}-\boldsymbol{\delta}_j^{(k)},\boldsymbol{X}_i^{(k)}-\boldsymbol{X}_j^{(k)}\right\rangle\\&=-\alpha\sum_{i=1}^{N-1}\sum_{j>i}^{N}\left\{\left\langle\boldsymbol{\delta}_i^{(k)},\boldsymbol{X}_i^{(k)}\right\rangle-\left\langle\boldsymbol{\delta}_i^{(k)},\boldsymbol{X}_j^{(k)}\right\rangle-\left\langle\boldsymbol{\delta}_j^{(k)},\boldsymbol{X}_i^{(k)}\right\rangle+\left\langle\boldsymbol{\delta}_j^{(k)},\boldsymbol{X}_j^{(k)}\right\rangle\right\}\\&=-\alpha(N-1)\sum_{i=1}^{N}\left\langle\boldsymbol{\delta}_i^{(k)},\boldsymbol{X}_i^{(k)}\right\rangle+\alpha\sum_{i=1}^{N}\left\langle\sum_{\substack{j\neq i\\ j=1}}^{N}\boldsymbol{\delta}_j^{(k)},\boldsymbol{X}_i^{(k)}\right\rangle\\&=-\alpha(N-1)\sum_{i=1}^{N}\left\langle\boldsymbol{\delta}_i^{(k)},\boldsymbol{X}_i^{(k)}\right\rangle-\alpha\sum_{i=1}^{N}\left\langle\boldsymbol{\delta}_j^{(k)},\boldsymbol{X}_i^{(k)}\right\rangle\\&=-\alpha N\sum_{i=1}^{N}\left\langle\boldsymbol{\delta}_i^{(k)},\boldsymbol{X}_i^{(k)}\right\rangle=-\alpha NV_d^{(k)}.\end{aligned} \tag{20}$$

Hence Eq. (19) can be rewritten as:

$$\begin{aligned}\Delta V_{[1]} = &-\alpha N V_{\mathrm{d}}^{(k)} \\ &+ \sum_{\delta_{\mathrm{ij}}^{(k)}>0} \sum_{\delta_{\mathrm{ij}}^{(k+1)}=0} \left\langle d_{\mathrm{ij}}^{(k+1)} \boldsymbol{n}_{\mathrm{ij}}^{(k+1)} - 2r\boldsymbol{n}_{\mathrm{ij}}^{(k)}, d_{\mathrm{ij}}^{(k)} \boldsymbol{n}_{\mathrm{ij}}^{(k)} \right\rangle \\ &+ \sum_{\delta_{\mathrm{ij}}^{(k)}=0} \sum_{\delta_{\mathrm{ij}}^{(k+1)}>0} \left\langle 2r\boldsymbol{n}_{\mathrm{ij}}^{(k+1)} - d_{\mathrm{ij}}^{(k)} \boldsymbol{n}_{\mathrm{ij}}^{(k)}, d_{\mathrm{ij}}^{(k)} \boldsymbol{n}_{\mathrm{ij}}^{(k)} \right\rangle \\ &+ \sum_{\delta_{\mathrm{ij}}^{(k)}>0} \sum_{\delta_{\mathrm{ij}}^{(k+1)}>0} \left\langle 2r\boldsymbol{n}_{\mathrm{ij}}^{(k+1)} - 2r\boldsymbol{n}_{\mathrm{ij}}^{(k)}, d_{\mathrm{ij}}^{(k)} \boldsymbol{n}_{\mathrm{ij}}^{(k)} \right\rangle .\end{aligned} \tag{21}$$

Notice that in Eq. (21), for non-zero overlaps, the third and fourth terms are negative and the second term can be either positive or negative. Under the small step size assumption, the majority of the inter-sphere overlaps will not be completely eliminated after one move ($\delta_{\mathrm{ij}}^{(k)}>0$, $\delta_{\mathrm{ij}}^{(k+1)}>0$). Therefore, the negative fourth term is dominant compared with the second term. For example, for an initially uniformly sampled sphere packing with 10,000 spheres within a cube at 60% packing fraction (step size $\alpha<0.5$), there is

$$\left| \sum_{\delta_{\mathrm{ij}}^{(k)}>0} \sum_{\delta_{\mathrm{ij}}^{(k+1)}>0} \left\langle 2r\boldsymbol{n}_{\mathrm{ij}}^{(k+1)} - 2r\boldsymbol{n}_{\mathrm{ij}}^{(k)}, d_{\mathrm{ij}}^{(k)} \boldsymbol{n}_{\mathrm{ij}}^{(k)} \right\rangle \right| > 4 \left| \sum_{\delta_{\mathrm{ij}}^{(k)}>0} \sum_{\delta_{\mathrm{ij}}^{(k+1)}=0} \left\langle d_{\mathrm{ij}}^{(k+1)} \boldsymbol{n}_{\mathrm{ij}}^{(k+1)} - 2r\boldsymbol{n}_{\mathrm{ij}}^{(k)}, d_{\mathrm{ij}}^{(k)} \boldsymbol{n}_{\mathrm{ij}}^{(k)} \right\rangle \right| .$$

Hence for a many sphere system with uniform initial sphere position sampling and using a small QDM step size, we have

$$\begin{aligned}&\sum_{\delta_{\mathrm{ij}}^{(k)}>0} \sum_{\delta_{\mathrm{ij}}^{(k+1)}=0} \left\langle d_{\mathrm{ij}}^{(k+1)} \boldsymbol{n}_{\mathrm{ij}}^{(k+1)} - 2r\boldsymbol{n}_{\mathrm{ij}}^{(k)}, d_{\mathrm{ij}}^{(k)} \boldsymbol{n}_{\mathrm{ij}}^{(k)} \right\rangle \\ &+ \sum_{\delta_{\mathrm{ij}}^{(k)}=0} \sum_{\delta_{\mathrm{ij}}^{(k+1)}>0} \left\langle 2r\boldsymbol{n}_{\mathrm{ij}}^{(k+1)} - d_{\mathrm{ij}}^{(k)} \boldsymbol{n}_{\mathrm{ij}}^{(k)}, d_{\mathrm{ij}}^{(k)} \boldsymbol{n}_{\mathrm{ij}}^{(k)} \right\rangle \\ &+ \sum_{\delta_{\mathrm{ij}}^{(k)}>0} \sum_{\delta_{\mathrm{ij}}^{(k+1)}>0} \left\langle 2r\boldsymbol{n}_{\mathrm{ij}}^{(k+1)} - 2r\boldsymbol{n}_{\mathrm{ij}}^{(k)}, d_{\mathrm{ij}}^{(k)} \boldsymbol{n}_{\mathrm{ij}}^{(k)} \right\rangle \\ &< 0.\end{aligned} \tag{22}$$

Finally we can obtain

$$\begin{aligned}\Delta V_{[1]} = &-\alpha N V_{\mathrm{d}}^{(k)} + \\ &\sum_{\delta_{\mathrm{ij}}^{(k)}>0} \sum_{\delta_{\mathrm{ij}}^{(k+1)}=0} \left\langle d_{\mathrm{ij}}^{(k+1)} \boldsymbol{n}_{\mathrm{ij}}^{(k+1)} - 2r\boldsymbol{n}_{\mathrm{ij}}^{(k)}, d_{\mathrm{ij}}^{(k)} \boldsymbol{n}_{\mathrm{ij}}^{(k)} \right\rangle + \\ &\sum_{\delta_{\mathrm{ij}}^{(k)}=0} \sum_{\delta_{\mathrm{ij}}^{(k+1)}>0} \left\langle 2r\boldsymbol{n}_{\mathrm{ij}}^{(k+1)} - d_{\mathrm{ij}}^{(k)} \boldsymbol{n}_{\mathrm{ij}}^{(k)}, d_{\mathrm{ij}}^{(k)} \boldsymbol{n}_{\mathrm{ij}}^{(k)} \right\rangle + \\ &\sum_{\delta_{\mathrm{ij}}^{(k)}>0} \sum_{\delta_{\mathrm{ij}}^{(k+1)}>0} \left\langle 2r\boldsymbol{n}_{\mathrm{ij}}^{(k+1)} - 2r\boldsymbol{n}_{\mathrm{ij}}^{(k)}, d_{\mathrm{ij}}^{(k)} \boldsymbol{n}_{\mathrm{ij}}^{(k)} \right\rangle \\ &< -\alpha N V_{\mathrm{d}}^{(k)},\end{aligned} \tag{23}$$

for non-zero overlaps at small step sizes.

Inequality (23) shows that for the unconstrained case, QDM will generate a descending sequence of system potentials which converges at an exponential rate related to the step size α. Although a larger step size would result in faster convergence, it will also result in larger summed overlaps after one move and make the first order term $\Delta V_{[1]}$ non-dominant over the second order term $\Delta V_{[2]}$ which is positive most of the time, especially at the initial stage when

$\sum_{i=1}^{N}\left\langle \boldsymbol{\delta}_{\mathrm{i}}^{(k+1)}, \boldsymbol{\delta}_{\mathrm{i}}^{(k)} \right\rangle$ itself is large. For large step size, many inter-sphere overlaps will be eliminated after one move (on the other side, many new overlaps will occur after one move), which will make inequality (23) invalid. The combination of the above factors could lead to divergence. The upper limit of step size will be discussed in the next section.

3-2 Stability of constrained situation

The constrained situations in this section refer to the even dense packing with active boundary constraints, which usually have a packing fraction well above 55% [3, 6] for large systems (and smaller than the random close packing limit which is around 64%). Due to the projection operation in the constrained cases, the analysis approach used above for the unconstrained case does not work for the constrained situation. A convex analysis approach using the 2-potential function V_2 is employed to derive the stability condition for the constrained situation. Although the analysis approach is different from the unconstrained case, the analysis here still benefits from the unconstrained case analysis by using Lemma 1 and several other facts and equations.

In order to use the convex analysis approach, it requires that the target function is convex. However, $V(\boldsymbol{X})$ is not a globally convex function. Consider a two sphere packing problem for example. Figure 1a shows two spheres with radii of 0.5 packed within the region [-1.2 1.2], and the potential function is shown in Fig. 1b. From the figure we can see that there are two basins for $V(\boldsymbol{X})$ and the peak of the basin corresponds with complete overlap between the two spheres which is a singular situation that cannot be handled by QDM. The potential function is not convex globally but convex within each basin.

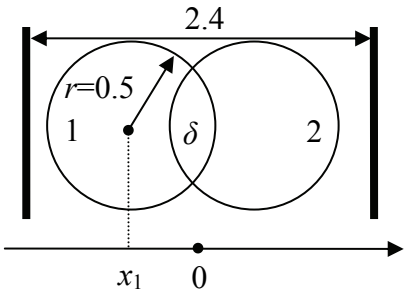

(a) Two sphere packing in 1-D

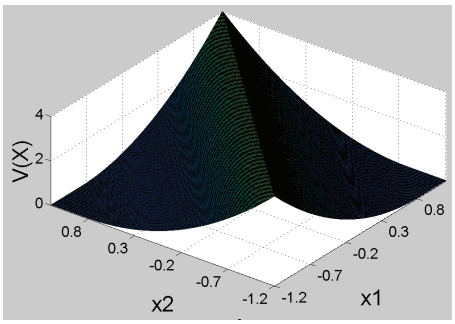

(b) $V(\boldsymbol{X})$ for two-sphere 1-D packing

Figure 1. Non-convexity and local convexity demonstration for potential function $V(\boldsymbol{X})$.

Jamming is a possible phenomenon for densely packed equal spheres within a container, which starts locally when the packing fraction is close to the random close packing limit and may exist globally when the packing fraction is around 64%. Jamming also exists in the general collective overlap-eliminating sphere packing process. For a globally jammed state $\boldsymbol{X}^{\mathrm{J}}$, it does not share any convex basin with any overlap free state X* and also cannot be handled by QDM because none of the spheres can move any further to an overlap free state. If we

define the convergence rate of QDM as $\rho^{(k)} = V^{(k)}(\boldsymbol{X})/V^{(k-1)}(\boldsymbol{X})$, then from Fig. 2 we can see that as the packing fraction approaches the random close packing limit, the convergence performance deteriorates due to larger overall overlap. When the packing fraction is higher than 63.5%, QDM would be divergent (average $\rho^{(k)}$ is greater than 1) due to the occurrence of global jamming. The packing fraction in this work is limited below 63.5% to avoid a possible jammed state. In practice, for non-jammed packing, a uniform sampling for initial sphere positions can mostly avoid extreme inter-sphere overlaps such as complete overlap between two spheres or near-complete overlap among multiple spheres. Hence there is usually at least one overlap-free state within the convex potential basin that includes the initial state.

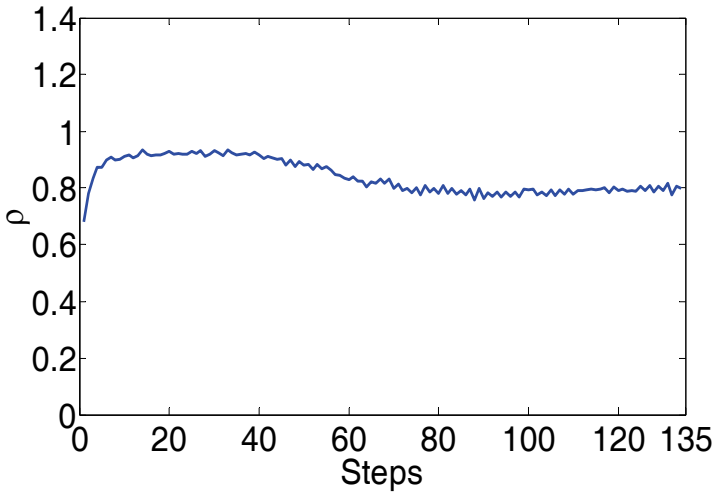

(a) φ=0.580

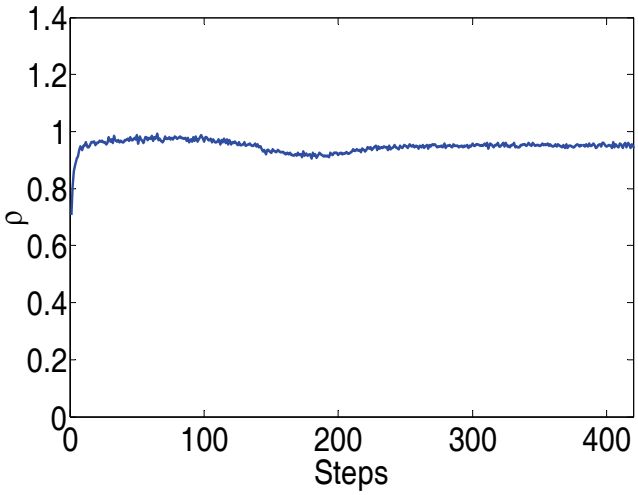

(b) φ=0.610

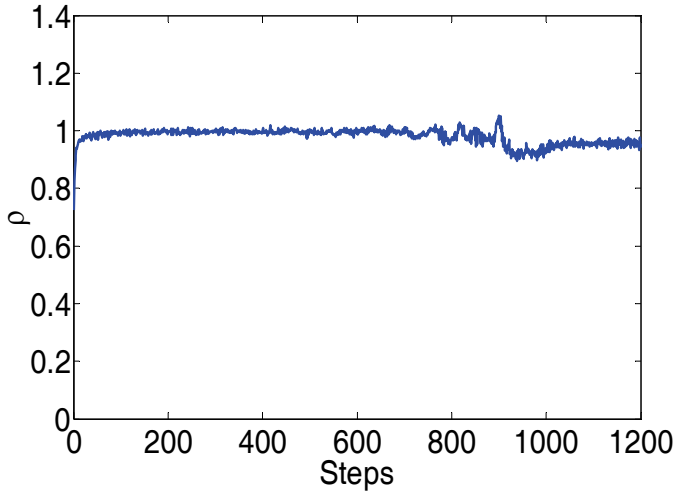

(c) φ=0.625

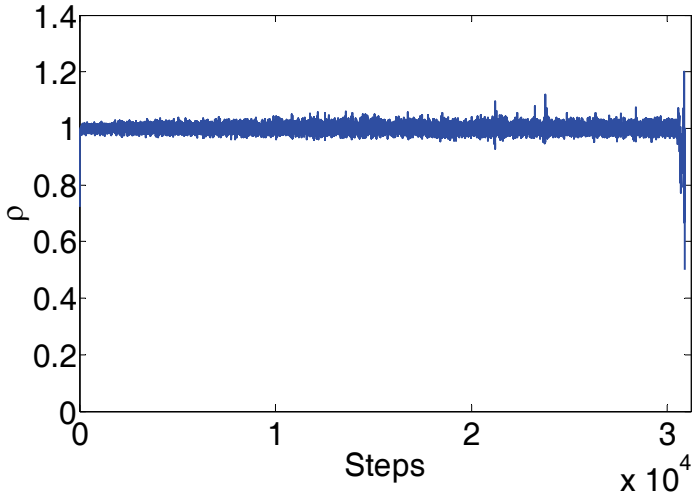

(d) φ=0.635

Figure 2. Convergence rates at different packing fractions for α=0.86.

The analysis in this section provides proof that, starting from an initial state which shares at least one overlap-free state $\boldsymbol{X}^*$ within the same convex basin of 2-potential function, QDM can converge to within a small finite range (local stability) to $\boldsymbol{X}^*$.

Now for the $(k+1)^{th}$ step, the Euclidean distance to the optimal value can be written as:

$$\begin{aligned} \left\|\boldsymbol{X}^{(k+1)}-\boldsymbol{X}^*\right\|^2 &= \left\|\boldsymbol{X}^{(k)}+\alpha\boldsymbol{\delta}^{(k)}-\boldsymbol{X}^*\right\|^2 \\ &= \left\|\boldsymbol{X}^{(k)}-\boldsymbol{X}^*\right\|^2 + 2\alpha\boldsymbol{\delta}^{(k)T}(\boldsymbol{X}^{(k)}-\boldsymbol{X}^*)+\alpha^2\left\|\boldsymbol{\delta}^{(k)}\right\|^2. \end{aligned} \tag{24}$$

From Lemma 1, Eq. (24) can be rearranged as:

$$
\begin{aligned}
&\left\|\boldsymbol{X}^{(k+1)}-\boldsymbol{X}^{*}\right\|^{2} \\
&=\left\|\boldsymbol{X}^{(k)}-\boldsymbol{X}^{*}\right\|^{2}+2\alpha(\sum_{i=1}^{N}\left\langle\boldsymbol{\delta}_{\mathrm{i}}^{(k)},\boldsymbol{X}_{\mathrm{i}}^{(k)}\right\rangle-\sum_{i=1}^{N}\left\langle\boldsymbol{\delta}_{\mathrm{i}}^{(k)},\boldsymbol{X}^{*}\right\rangle)+\alpha^{2}\left\|\boldsymbol{\delta}^{(k)}\right\|^{2} \\
&=\left\|\boldsymbol{X}^{(k)}-\boldsymbol{X}^{*}\right\|^{2}+2\alpha(\sum_{i=1}^{N-1}\sum_{j>i}^{N}\delta_{\mathrm{ij}}^{(k)}d_{\mathrm{ij}}^{(k)}-\sum_{i=1}^{N-1}\sum_{j>i}^{N}\left\langle\delta_{\mathrm{ij}}\frac{\boldsymbol{X}_{\mathrm{i}}-\boldsymbol{X}_{\mathrm{j}}}{d_{\mathrm{ij}}},\boldsymbol{X}_{\mathrm{i}}^{*}-\boldsymbol{X}_{\mathrm{j}}^{*}\right\rangle)+\alpha^{2}\left\|\boldsymbol{\delta}^{(k)}\right\|^{2} \\
&=\left\|\boldsymbol{X}^{(k)}-\boldsymbol{X}^{*}\right\|^{2}+2\alpha(\sum_{i=1}^{N-1}\sum_{j>i}^{N}\delta_{\mathrm{ij}}^{(k)}d_{\mathrm{ij}}^{(k)}-\sum_{i=1}^{N-1}\sum_{j>i}^{N}\delta_{\mathrm{ij}}^{(k)}d_{\mathrm{ij}}^{*}\cos(\boldsymbol{d}_{\mathrm{ij}}^{(k)},\boldsymbol{d}_{\mathrm{ij}}^{*}))+\alpha^{2}\left\|\boldsymbol{\delta}^{(k)}\right\|^{2} \\
&=\left\|\boldsymbol{X}^{(k)}-\boldsymbol{X}^{*}\right\|^{2}+2\alpha(\sum_{i=1}^{N-1}\sum_{j>i}^{N}\delta_{\mathrm{ij}}^{(k)}(d_{\mathrm{ij}}^{(k)}-d_{\mathrm{ij}}^{*}\cos(\boldsymbol{d}_{\mathrm{ij}}^{(k)},\boldsymbol{d}_{\mathrm{ij}}^{*})))+\alpha^{2}\left\|\boldsymbol{\delta}^{(k)}\right\|^{2}.
\end{aligned}
\tag{25}
$$

For the $\delta_{\mathrm{ij}}^{(k)}[d_{\mathrm{ij}}^{(k)}-d_{\mathrm{ij}}^{*}\cos(\boldsymbol{d}_{\mathrm{ij}}^{(k)},\boldsymbol{d}_{\mathrm{ij}}^{*})]$ term in Eq. (25), because $\boldsymbol{d}_{\mathrm{ij}}^{(k)}$ has different expressions when $\delta_{\mathrm{ij}}^{(k)}=0$ and $\delta_{\mathrm{ij}}^{(k)}>0$, we need to discuss these two situations separately.
If $\delta_{\mathrm{ij}}^{(k)}>0$, there is

$$
\begin{aligned}
&\delta_{\mathrm{ij}}^{(k)}[d_{\mathrm{ij}}^{(k)}-d_{\mathrm{ij}}^{*}\cos(\boldsymbol{d}_{\mathrm{ij}}^{*},\boldsymbol{d}_{\mathrm{ij}}^{(k)})] \\
&=\delta_{\mathrm{ij}}^{(k)}[2r-\delta_{\mathrm{ij}}^{(k)}-d_{\mathrm{ij}}^{*}\cos(\boldsymbol{d}_{\mathrm{ij}}^{*},\boldsymbol{d}_{\mathrm{ij}}^{(k)})] \\
&=\delta_{\mathrm{ij}}^{(k)}[-\delta_{\mathrm{ij}}^{(k)}+2r-d_{\mathrm{ij}}^{*}\cos(\boldsymbol{d}_{\mathrm{ij}}^{*},\boldsymbol{d}_{\mathrm{ij}}^{(k)})] \\
&\le\delta_{\mathrm{ij}}^{(k)}[-\delta_{\mathrm{ij}}^{(k)}+d_{\mathrm{ij}}^{*}-d_{\mathrm{ij}}^{*}\cos(\boldsymbol{d}_{\mathrm{ij}}^{*},\boldsymbol{d}_{\mathrm{ij}}^{(k)})] \\
&=\delta_{\mathrm{ij}}^{(k)}[-\delta_{\mathrm{ij}}^{(k)}+d_{\mathrm{ij}}^{*}(1-\cos(\boldsymbol{d}_{\mathrm{ij}}^{*},\boldsymbol{d}_{\mathrm{ij}}^{(k)}))] \\
&=-\delta_{\mathrm{ij}}^{(k)2}+d_{\mathrm{ij}}^{*}(1-\cos(\boldsymbol{d}_{\mathrm{ij}}^{*},\boldsymbol{d}_{\mathrm{ij}}^{(k)}))\delta_{\mathrm{ij}}^{(k)}.
\end{aligned}
\tag{26}
$$

In the third step of (26), the "=" is satisfied when $d_{\mathrm{ij}}^{*}=2r$.
Or if $\delta_{\mathrm{ij}}^{(k)}=0$, then

$$
\begin{aligned}
&\delta_{\mathrm{ij}}^{(k)}[d_{\mathrm{ij}}^{(k)}-d_{\mathrm{ij}}^{*}\cos(\boldsymbol{d}_{\mathrm{ij}}^{*},\boldsymbol{d}_{\mathrm{ij}}^{(k)})] \\
&=0 \\
&=-\delta_{\mathrm{ij}}^{(k)2}+d_{\mathrm{ij}}^{*}(1-\cos(\boldsymbol{d}_{\mathrm{ij}}^{*},\boldsymbol{d}_{\mathrm{ij}}^{(k)}))\delta_{\mathrm{ij}}^{(k)}.
\end{aligned}
$$

Hence (25) can be rewritten as

$$
\begin{aligned}
&\left\|\boldsymbol{X}^{(k+1)}-\boldsymbol{X}^{*}\right\|^{2} \\
&\le\left\|\boldsymbol{X}^{(k)}-\boldsymbol{X}^{*}\right\|^{2}+2\alpha\sum_{i=1}^{N-1}\sum_{j>i}^{N}(-\delta_{\mathrm{ij}}^{(k)2}+d_{\mathrm{ij}}^{*}(1-\cos(\boldsymbol{d}_{\mathrm{ij}}^{*},\boldsymbol{d}_{\mathrm{ij}}^{(k)}))\delta_{\mathrm{ij}}^{(k)})+\alpha^{2}\left\|\boldsymbol{\delta}^{(k)}\right\|^{2} \\
&=\left\|\boldsymbol{X}^{(k)}-\boldsymbol{X}^{*}\right\|^{2}-2\alpha V(\boldsymbol{X}^{(k)})+2\alpha\sum_{i=1}^{N-1}\sum_{j>i}^{N}(d_{\mathrm{ij}}^{*}(1-\cos(\boldsymbol{d}_{\mathrm{ij}}^{*},\boldsymbol{d}_{\mathrm{ij}}^{(k)}))\delta_{\mathrm{ij}}^{(k)})+\alpha^{2}\left\|\boldsymbol{\delta}^{(k)}\right\|^{2}.
\end{aligned}
\tag{27}
$$

It should be pointed out that all the norms in Eq. (27) are 2-norms based on the original equation (24). Based on triangle inequality, we obtain:

$$\begin{aligned}\left\|\boldsymbol{\delta}^{(k)}\right\|^2 &= \sum_{i=1}^{N}\left\|\boldsymbol{\delta}_{\mathrm{i}}^{(k)}\right\|^2 = \sum_{i=1}^{N}\left\|\sum_{\substack{j=1\\ j\neq i}}^{N}\boldsymbol{\delta}_{\mathrm{ij}}^{(k)}\right\|^2 \\ &\le \sum_{i=1}^{N}(\sum_{\substack{j=1\\ j\neq i}}^{N}\delta_{\mathrm{ij}}^{(k)})^2 = 2V(\boldsymbol{X}^{(k)}) + 2\sum_{i=1}^{N}\sum_{\substack{j=1\\ j\neq i}}^{N-1}\sum_{\substack{l=1\\ l\neq i\\ l>j}}^{N}\delta_{\mathrm{ij}}^{(k)}\delta_{\mathrm{il}}^{(k)},\end{aligned} \tag{28}$$

where the "=" can be satisfied when $\left\|\boldsymbol{\delta}_{\mathrm{i}}^{(k)}\right\| = \sum_{\substack{j=1\\ j\neq i}}^{N}\delta_{\mathrm{ij}}^{(k)}$ for any i, meaning that for any sphere i, the inter-sphere overlaps are aligned along the same direction. This further implies that sphere i overlaps with no more than one spheres. Hence the second term in (16), which is non-negative for any i, j and l, equals zero for multi-sphere systems when "=" is satisfied. Inequality (27) can be proceeded as:

$$\begin{aligned}&\left\|\boldsymbol{X}^{(k+1)} - \boldsymbol{X}^*\right\|^2 \\ &\le \left\|\boldsymbol{X}^{(k)} - \boldsymbol{X}^*\right\|^2 + 2\alpha\sum_{i=1}^{N\text{-}1}\sum_{j>i}^{N}(-\delta_{\mathrm{ij}}^{(k)2} + 2r(1-\cos(\boldsymbol{d}_{\mathrm{ij}}^{\,*}, \boldsymbol{d}_{\mathrm{ij}}^{(k)}))\delta_{\mathrm{ij}}^{(k)}) + \alpha^2\left\|\boldsymbol{\delta}^{(k)}\right\|^2 \\ &= \left\|\boldsymbol{X}^{(k)} - \boldsymbol{X}^*\right\|^2 - 2\alpha(1-\alpha)V(\boldsymbol{X}^{(k)}) + \\ &\quad 2\alpha\sum_{i=1}^{N\text{-}1}\sum_{j>i}^{N}(d_{\mathrm{ij}}^{\,*}(1-\cos(\boldsymbol{d}_{\mathrm{ij}}^{\,*}, \boldsymbol{d}_{\mathrm{ij}}^{(k)}))\delta_{\mathrm{ij}}^{(k)}) + 2\alpha^2\sum_{i=1}^{N}\sum_{\substack{j=1\\ j\neq i}}^{N-1}\sum_{\substack{l=1\\ l\neq i\\ l>j}}^{N}\delta_{\mathrm{ij}}^{(k)}\delta_{\mathrm{il}}^{(k)}.\end{aligned} \tag{29}$$

Eq. (29) associates the distance to the final overlap-free state at the $(k+1)^{\text{th}}$ step ($\|\boldsymbol{X}^{(k+1)}\text{-}\boldsymbol{X}^*\|$) with that at the k^{th} step ($\|\boldsymbol{X}^{(k)}\text{-}\boldsymbol{X}^*\|$) which is the first term of the right hand side of Eq. (29). As we can see, the last two terms are non-negative. And since for all the inequalities by far, "=" can be satisfied under certain conditions, it requires that the second term in (29) be smaller than zero, otherwise the algorithm could be divergent. This necessary condition can be written as $\alpha(1\text{-}\alpha) \ge 0$ which yields $0 \le \alpha \le 1$. This important result shows that the critical step size for QDM should not exceed 1. In practice, the third term is non-negative and the step size should not be too close to 1 in order to maintain the convergence throughout the overlap elimination process, which can also be verified by 3-d packing examples shown in Fig. 3. Fig. 3 is a mono-dispersed sphere packing within a unit sphere container. By adjusting the sphere radius, we can study the relation between critical step size and the geometry size (represented by sphere number N). The figure shows that the critical step size α_{c} approaches 1 as the system size approaches infinity.

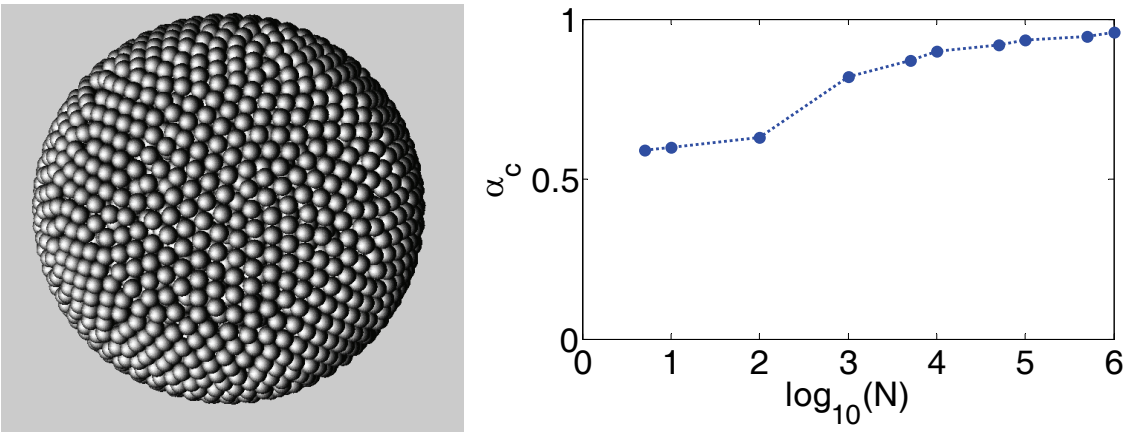

(a) Spherical packing geometry (b) Impact of sphere number N on K_d^c

Figure 3. Impact of system size (N) on upper limit of QDM step size α_c.

Applying the above inequality recursively from the 1st to the k^{th} step, we can obtain

$$\begin{aligned} 0 &\le \left\| \boldsymbol{X}^{(k+1)} - \boldsymbol{X}^* \right\|^2 \\ &\le \left\| \boldsymbol{X}^{(1)} - \boldsymbol{X}^* \right\|^2 - 2\alpha(1-\alpha)\sum_{l=1}^{k} V(\boldsymbol{X}^{(l)}) + \\ &\quad 2\alpha\sum_{s=1}^{k}\sum_{i=1}^{N-1}\sum_{j>i}^{N}(d_{ij}^{*}(1-\cos(\boldsymbol{d}_{ij}^{*},\boldsymbol{d}_{ij}^{(s)}))\delta_{ij}^{(s)}) + 2\alpha^2\sum_{s=1}^{k}\sum_{i=1}^{N}\sum_{\substack{j=1\\ j\neq i}}^{N-1}\sum_{\substack{l=1\\ l\neq i\\ l>j}}^{N}\delta_{ij}^{(s)}\delta_{il}^{(s)}. \end{aligned} \tag{30}$$

Using $\left\| \boldsymbol{X}^{(k+1)} - \boldsymbol{X}^* \right\|^2 \ge 0$, we have

$$\begin{aligned} &2\alpha(1-\alpha)\sum_{l=1}^{k} V(\boldsymbol{X}^{(l)}) \le \left\| X^{(1)} - X^* \right\|^2 + \\ &2\alpha\sum_{s=1}^{k}\sum_{i=1}^{N-1}\sum_{j>i}^{N}(d_{ij}^{*}(1-\cos(\boldsymbol{d}_{ij}^{*},\boldsymbol{d}_{ij}^{(s)}))\delta_{ij}^{(s)}) + 2\alpha^2\sum_{s=1}^{k}\sum_{i=1}^{N}\sum_{\substack{j=1\\ j\neq i}}^{N-1}\sum_{\substack{l=1\\ l\neq i\\ l>j}}^{N}\delta_{ij}^{(s)}\delta_{il}^{(s)}. \end{aligned} \tag{31}$$

Denote $V(\boldsymbol{X}^{(k)})_{best}$ as the minimum value among $V(\boldsymbol{X}^{(l)})$, l=1, 2, … k. Then there is:

$$\sum_{l=1}^{k} V(\boldsymbol{X}^{(l)}) \ge \sum_{l=1}^{k} \min_{1,2..k}(V(\boldsymbol{X}^{(l)})) = kV(\boldsymbol{X}^{(k)})_{best}. \tag{32}$$

Also we can see that $\sum_{i=1}^{N-1}\sum_{j>i}^{N}((1-\cos(\boldsymbol{d}_{ij}^{*},\boldsymbol{d}_{ij}^{(k)}))\delta_{ij}^{(k)}) \to 0$ and $\sum_{i=1}^{N}\sum_{\substack{j=1\\ j\neq i}}^{N-1}\sum_{\substack{l=1\\ l\neq i\\ l>j}}^{N}\delta_{ij}^{(s)}\delta_{il}^{(s)} \to 0$ as the algorithm converges. Hence both of them are bounded and non-negative for a converged process. Denote $F^{(k)}$ and $G^{(k)}$ as the maximum value of $\sum_{i=1}^{N-1}\sum_{j>i}^{N}(d_{ij}^{*}(1-\cos(\boldsymbol{d}_{ij}^{*},\boldsymbol{d}_{ij}^{(k)}))\delta_{ij}^{(k)})$

and $\sum_{i=1}^{N}\sum_{\substack{j=1\\ j\neq i}}^{N-1}\sum_{\substack{l=1\\ l\neq i\\ l>j}}^{N}\delta_{ij}^{(s)}\delta_{il}^{(s)}$, respectively, from the 1st to the k^{th} step, which can be interpreted as another measure of overlap extent through the k^{th} step. We now have the inequality (31) as

$$\begin{aligned} V(\boldsymbol{X}^{(k)})_{best} &\le \frac{\left\|X^{(1)}-X^{*}\right\|^2}{2k\alpha(1-\alpha)}+\frac{kF^{(k)}}{k(1-\alpha)}+\frac{k\alpha G^{(k)}}{k(1-\alpha)} \\ &= \frac{\left\|\boldsymbol{X}^{(1)}-\boldsymbol{X}^{*}\right\|^2}{2k\alpha(1-\alpha)}+\frac{F^{(k)}+\alpha G^{(k)}}{(1-\alpha)} \\ &= U(\boldsymbol{X}^{(1)}). \end{aligned} \tag{33}$$

Now we obtain this upper bound function $U(\boldsymbol{X})$ which is easier to analyze compared with the original potential function $V(\mathbf{X})$.

Up until now, the boundary constraints have not been considered. We can denote $\boldsymbol{Z}^{(k+1)}$ (a state before wall pushes spheres back) as:

$$\begin{aligned} \boldsymbol{Z}^{(k+1)} &= \boldsymbol{X}^{(k)}+\alpha^{(k)}\boldsymbol{\delta}^{(k)} \\ \boldsymbol{X}^{(k+1)} &= P(\boldsymbol{Z}^{(k+1)}) \end{aligned} \tag{34}$$

If we denote $\boldsymbol{Z}_{\|}=P(\boldsymbol{Z})$ and $\boldsymbol{Z}_{\perp}=\boldsymbol{Z}-\boldsymbol{Z}_{\|}$, then there is following Lemma 2 [16]:

Lemma 2:

For $P(\bullet):\mathbb{R}^{3N}\to\boldsymbol{C}$, there is $\left\langle \boldsymbol{Z}_{\perp},\boldsymbol{Z}_{\|}-\boldsymbol{X}\right\rangle \ge 0$.

By using Lemma 2 , we can obtain following important non-expansion properties of projection.

Lemma 3:

For $P(\bullet):\mathbb{R}^{3N}\to\boldsymbol{C}$, there is $\left\|P(Z)-\boldsymbol{X}\right\|\le\left\|Z-\boldsymbol{X}\right\|$, for $\forall\boldsymbol{Z}\in\mathbb{R}^{3N}$, $\boldsymbol{X}\in\boldsymbol{C}$.

Proof:

1) If $\boldsymbol{Z}\in\boldsymbol{C}$, $\left\|P(\boldsymbol{Z})-\boldsymbol{X}\right\|=\left\|\boldsymbol{Z}-\boldsymbol{X}\right\|$.

2) If $\boldsymbol{Z}\notin\boldsymbol{C}$, then

$$\begin{aligned} \left\|P(\boldsymbol{Z})-\boldsymbol{X}\right\|^2 &= (P(\boldsymbol{Z})-\boldsymbol{X})^T(P(\boldsymbol{Z})-\boldsymbol{X}) \\ &= \left\langle P(\boldsymbol{Z}),P(\boldsymbol{Z})\right\rangle-2\left\langle P(\boldsymbol{Z}),\boldsymbol{X}\right\rangle+\left\langle \boldsymbol{X},\boldsymbol{X}\right\rangle \\ &= \left\langle \boldsymbol{Z}_{\|},\boldsymbol{Z}_{\|}\right\rangle-2\left\langle \boldsymbol{Z}_{\|},\boldsymbol{X}\right\rangle+\left\langle \boldsymbol{X},\boldsymbol{X}\right\rangle. \end{aligned}$$

According to Lemma 2, $\left\langle \boldsymbol{Z}_{\perp},\boldsymbol{Z}_{\|}-\boldsymbol{X}\right\rangle\ge 0$. Hence:

$$\begin{aligned}\|P(\boldsymbol{Z})-\boldsymbol{X}\|^2 &\le \langle \boldsymbol{Z}_{\parallel},\boldsymbol{Z}_{\parallel}\rangle - 2\langle \boldsymbol{Z}_{\parallel},\boldsymbol{X}\rangle + \langle \boldsymbol{X},\boldsymbol{X}\rangle + 2\langle \boldsymbol{Z}_{\perp},\boldsymbol{Z}_{\parallel}-\boldsymbol{X}\rangle + \langle \boldsymbol{Z}_{\perp},\boldsymbol{Z}_{\perp}\rangle \\ &= \langle \boldsymbol{Z}_{\parallel}+\boldsymbol{Z}_{\perp},\boldsymbol{Z}_{\parallel}+\boldsymbol{Z}_{\perp}\rangle - 2\langle \boldsymbol{Z}_{\parallel}+\boldsymbol{Z}_{\perp},\boldsymbol{X}\rangle + \langle \boldsymbol{X},\boldsymbol{X}\rangle \\ &= \|\boldsymbol{Z}-\boldsymbol{X}\|^2 .\end{aligned}$$

Lemma 3 can be interpreted by recognizing that the projection operation will not expand the distance between the two points. With the help of this lemma we can finalize the stability proof for the constrained situation:

$$\left\|\boldsymbol{X}^{(k+1)}-\boldsymbol{X}^{*}\right\|^2 \le \left\|\boldsymbol{Z}^{(k+1)}-\boldsymbol{X}^{*}\right\|^2 \le \left\|\boldsymbol{X}^{(k)}-\boldsymbol{X}^{*}\right\|^2 + 2\alpha\boldsymbol{\delta}^{(k)T}(\boldsymbol{X}^{(k)}-\boldsymbol{X}^{*}) + \alpha^2\left\|\boldsymbol{\delta}^{(k)}\right\|^2 \qquad (35)$$

The same upper bound function $U(\boldsymbol{X}^{(1)})$ is obtained from Eq. (35) as that in Eq. (33). By now the stability proof for the constrained case is finished.

4. Analysis and Numerical Results

For constrained situations, the analytical approach leads to an upper bound function for the system potential, defined by U, which is smooth and has a simpler form compared with the potential function. The term $\|\boldsymbol{X}^{(1)}\text{-}\boldsymbol{X}^{*}\|^2$ can be interpreted as the distance between the initial state and the final overlap-free configuration, which is a finite value. From (33) we can see that, as $k\rightarrow\infty$, $V(\boldsymbol{X}^{(k)})_{best}$ converges sublinearly to within $[0, \frac{F^{(k)}+\alpha G^{(k)}}{(1-\alpha)}]$ which is controlled by the step size α and the initial state ($F^{(k)}$ and $G^{(k)}$ are functions of the initial state). Hence the QDM is locally stable for constrained non-jammed packing.

In fact, the upper bound function $U(\boldsymbol{X})$ is quite a conservative estimation. The comparison between the real convergence process and the $U(\boldsymbol{X})$ history is shown in Fig. 4 for a 25,000 sphere cube packing (61% packing fraction, α=0.88) in which sphere centers are initially generated by a uniform sampling.

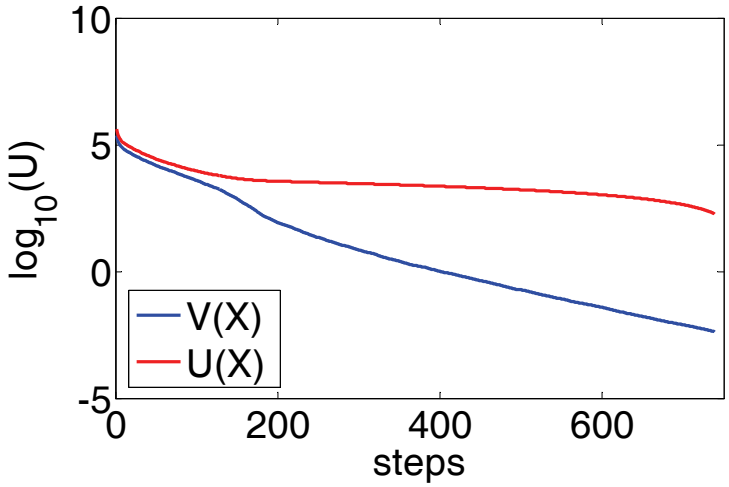

Figure 4. $V(\boldsymbol{X})$ and $U(\boldsymbol{X})$ history for QDM

From Fig. 4 it can be seen that, while the $U(\boldsymbol{X})$ is still significantly large, the objective function $V(\boldsymbol{X})$ already decreases to a very small value. Hence the real convergence performance will be better compared with the analytical prediction.

Another important contribution from the analysis is the criteria for choosing key algorithm parameters such as the step size α. It is obvious that a larger step size results in faster overall overlap elimination for loose packing and can be clearly seen from the analysis of the unconstrained case. This also applies to dense packing which can be verified by a typical 61% dense constrained packing shown in Fig. 5a. Therefore α>0.5 is always suggested for better efficiency. However, for an initial state with significant inter-sphere overlaps, this is not true at the initial stage of overlap eliminating process. From Eq. (33) it can be seen that the upper bound function $U(\boldsymbol{X})$ consists of two parts: $\frac{\left\|\boldsymbol{X}^{(1)}-\boldsymbol{X}^{*}\right\|^{2}}{2k\alpha(1-\alpha)}$, and $\frac{F^{(k)}+\alpha G^{(k)}}{(1-\alpha)}$. We can see that both parts are affected by the step size. For the first term (initial distance to equilibrium), smaller step size leads to smaller $U(\boldsymbol{X})$ hence faster convergence when the step size is greater than 0.5, and same for the second term which means that smaller step size will lead to a faster initial convergence and a smaller bounding region. This prediction is verified as shown in Fig. 5b (61% packing) and Fig. 5c (63.5% packing). For 63.5% packing the log-scale of $V(\boldsymbol{X})$ is not used in order to better show the oscillation of potential function due to higher packing fraction. From both figures we can see that, starting from a large overlap potential function generated by an initial uniform sampling, a larger step size leads to a slower initial convergence for both cases which is consistent with the theoretical prediction. This conclusion can also be drawn from the decomposition of system potentials' difference into 1st order term $\Delta V_{[1]}$ and 2nd order term $\Delta V_{[2]}$ (Eq. (14). In the initial stage of QDM, the summed overlap is large and hence a small step size should be used to keep $\Delta V_{[1]}$ over $\Delta V_{[2]}$ with a consequent quick descending process. But as the overall overlap arrives at a very small value, the 2nd order term is far less than the 1st order term even for large step sizes, and based on inequality (23), at this stage a larger step size will result in quicker convergence rate and an overall faster convergence history. Based on this analysis, a variable step size should be chosen to achieve high efficiency. At the initial state of the algorithm, a smaller step size should be adopted to reduce the overlap function quicker. When the potential function is very small ($V(\boldsymbol{X})$~1e3 for a ~1e4 sphere system), a larger step size should be chosen for a better performance at the final stage of the overlap-eliminating process.

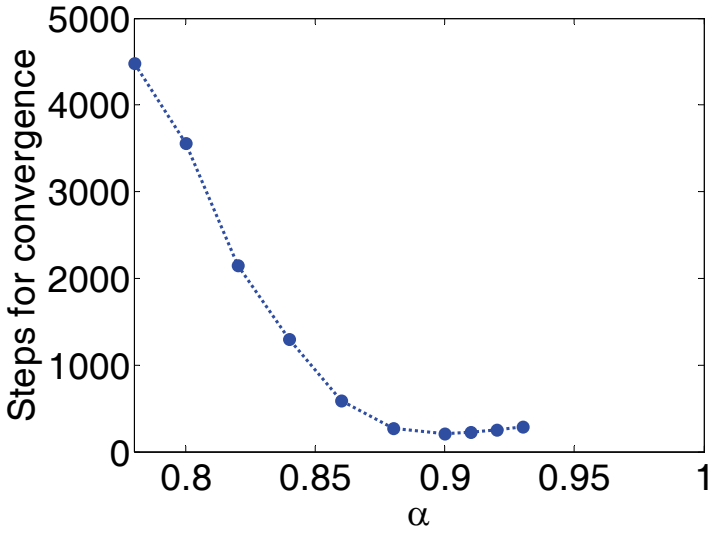

a) step size-convergence steps relation for 61% packing

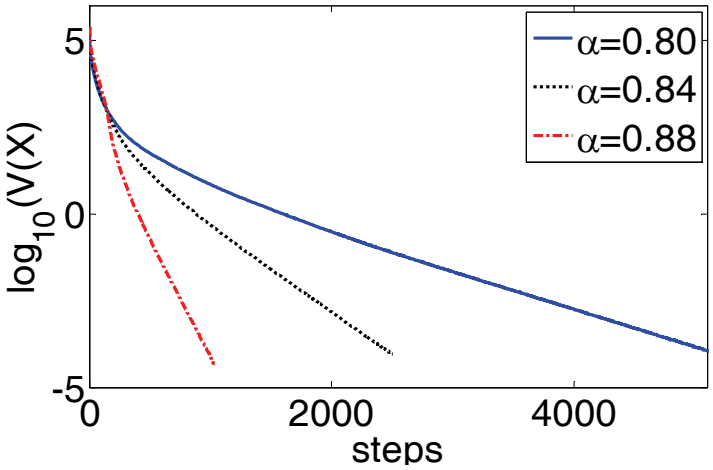

(b) Convergence history of $V(\boldsymbol{X})$ at α=0.8, 0.84 and 0.88 for 61% packing

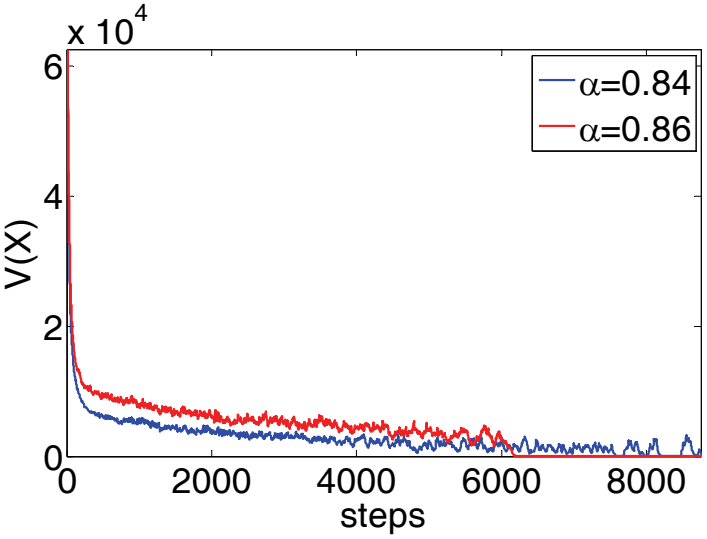

(c) Convergence history of $V(\boldsymbol{X})$ for 63.5% packing at α=0.84 and 0.86

Figure 5. Step size impact onto algorithm convergence

5. Conclusion

In this work, a theoretical analysis is provided for a collective rearrangement based sphere packing method, QDM, to prove the convergence for the unconstrained case and local stability for the dense constrained packing case. For the unconstrained/loose packing case, an exponential convergence rate of the potential function is obtained by analyzing the properties of the d-potential function. For the dense constrained packing case, an upper bound function with better analytical properties is obtained for the overlap-based 2-potential function using convex analysis. From the formulation of the upper bound function $U(\boldsymbol{X})$, a sublinear rate of convergence is predicted for QDM for dense constrained case, which is very important to estimate the runtime of QDM for large particle systems in granular material modeling. And the critical step size is predicted to be smaller than 1 which is numerically verified. Also it can be concluded that for both unconstrained and constrained cases, a smaller step size is favorable at the initial stage of the overlap-eliminating process to achieve better efficiency, while a larger step size at the final stage results in faster convergence. Although this analytical approach is based on a specific packing algorithm and mono-sized particle system, easy modifications can be made to enable this approach to apply to general collective packing algorithms and poly-dispersed systems. In addition, most of the analysis is based on general linear algebra. Hence this approach is promising to extend for the performance analysis for other similar collective overlap-eliminating algorithms such as Clarke's approach, which has been widely used but not yet theoretically analyzed.

References

[1] Widom, B. (1966) 'Random sequential addition of hard spheres to a volume.' *The Journal of Chemical Physics*,Vol. 44, pp.3888-3894.

[2] A.S. Clarke and Wiley, J.D. (1987) 'Numerical simulation of the dense random packing of a binary mixture of hard spheres: Amorphous metals,' *Physical Review B*, Vol. 35, pp.7350-7356.

[3] Jodrey, W.S. and Tory, E.M. (1985) 'Computer simulation of close random packing of equal spheres,' *Physical review A*, Vol. 32, pp.2347-2351.

[4] Mueller, G.E. (2005) 'Numerically packing spheres in cylinders,' *Powder technology*, Vol. 159, pp.105-110.

[5] Li, Y., and Ji, W. (2012) 'A collective dynamics-based method for initial pebble packing in pebble flow simulations,' *Nuclear Engineering and Design* Vol. 250, pp.229-236.

[6] Roozbahani, M.M. Huat, B.B.K. and Asadi, A. (2013) 'The effect of different random number distributions on the porosity of spherical particles,' *Advanced Powder Technology*, Vol. 24, pp.26–35.

[7] Shi, Y. and Zhang, Y. (2008) 'Simulation of random packing of spherical particles with different size distributions,' *Applied Physics A*, Vol. 92, pp.621-626.

[8] Goldrein, H. T. et al. (2002) 'The study of internal deformation fields in granular materials using 3D digital speckle X-ray flash photography,' *Shock compression of condensed*

matter, Vol. 620, pp.1105-1108.
[9] Arthur, J. R. F., et al. (1977) 'Plastic deformation and failure in granular media,' *Geotechnique*, Vol. 27, pp.53-74
[10] Ottino, J. M. and Khakhar, D.V. (2000) 'Mixing and segregation of granular materials,' *Annual Review of Fluid Mechanics*, Vol. 32, pp.55-91.
[11] Mishra, B. K. and Rajamani, R.K. (1992) 'The discrete element method for the simulation of ball mills,' *Applied Mathematical Modelling*, Vol. 16, pp.598-604.
[12] Li, Y. and Ji, W. (2013) 'Pebble Flow and Coolant Flow Analysis Based on a Fully Coupled Multi-Physics Model,' *Nuclear Science and Engineering*, Vol. 173, pp.150-162
[13] Li, Y. and Ji, W. (2013) 'Acceleration of Coupled Granular Flow and Fluid Flow Simulations in Pebble Bed Energy Systems,' *Nuclear Engineering and Design*, Vol. 258, pp. 275-283.
[14] Berryman, J.G. (1983) 'Random close packing of hard spheres and disks,' *Physical Review A*, Vol. 27, pp.1053-1061.
[15] Uhler, Caroline. and Wright, S.J. (2012) 'Packing ellipsoids with overlap,' *arXiv preprint arXiv:1204.0235*.
[16] Hiriart-Urruty, J.B. and Lemaréchal, C. (2001) *Fundamentals of convex analysis*. Berlin: Springer-Verlag. ISBN 978-3-540-42205-1